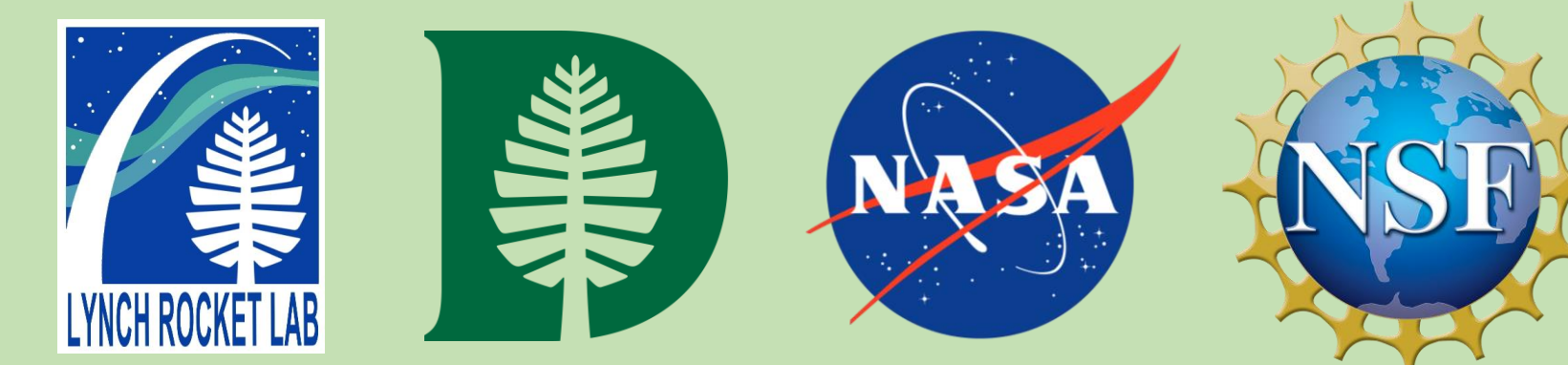


Auroral System Science - Multifluid 3D GEMINI Simulations of Auroral Arc Ionospheric Current Closure



Jules van Irsel¹, Edward W. McManus¹, Meghan Burleigh², Kristina A. Lynch¹, Matthew D. Zettergren³

¹Department of Physics, Dartmouth College; ²Space Science Division, Naval Research Laboratory; ³Physical Sciences Department, Embry-Riddle Aeronautical University

Background

- Local coupling of the ionosphere and magnetosphere (MI) is an open area of study (Wolf, 1975; Cowley, 2000; Lotko 2004; Amm et al. 2008).
- The magnetosphere demands self-consistent topside maps of field-aligned current (FAC) and $\mathbf{E} \times \mathbf{B}$ plasma flow that agree with ionospheric conductivity patterns created by associated charged particle arc precipitation.
- Discrete auroral precipitation provided by the auroral acceleration region has relatively local morphology to which the ionospheric conductivity is highly sensitive.
- Quasi-static ionospheric plasma flow, FAC, and conductivity is related through Eq. 6.12 in Kelley (2009):

$$j_{\parallel} = \Sigma_P(\nabla_{\perp} \cdot \mathbf{E}) + \mathbf{E} \cdot \nabla_{\perp} \Sigma_P + (\mathbf{E} \times \hat{\mathbf{b}}) \cdot \nabla_{\perp} \Sigma_H \quad (1)$$

- with j_{\parallel} being a horizontal 2D map of FAC at the topside ionosphere, Σ_P and Σ_H being the height-integrated Pedersen and Hall conductivities, and \mathbf{E} being the ionospheric electric field.
- I.e., ionospheric topside FAC contributions include:
 - Diverging electric fields (flow shear)
 - Across-arc Σ_P gradients
 - Along-arc Σ_H gradients
 - For sheet-like (latitudinally narrow, longitudinally aligned) arcs, finding self-consistent solutions to this is relatively well-posed (Marghitu, 2012).
 - For sheet-like arcs along-arc gradients are minimal and the $\nabla_{\perp} \Sigma_H$ term is often ignored.

Problem

- We want to find **physical, self-consistent solutions** to the ionospheric **current continuity** equation using 3D modelling for **less idealized** discrete auroral arc systems.
- In this, we want to provide insight into the role the ionosphere plays in MI coupling.
- Specifically, we aim to better understand the portions of FAC closed by Pedersen currents (which produce Joule heating) versus Hall currents (which are non-dissipative) in such cases (Kaeppler et al., 2012).
- How does the ionosphere act as a load to a magnetospheric generator?

Approach

- We use multi-fluid model runs provided by GEMINI (Zettergren & Semeter, 2012; Zettergren & Snively, 2019). For details see github.com/gemini3d.
- This model is state-of-the-art and can simulate the ionosphere at auroral arc scales (see Figure 1).
- This model solves for static current continuity to account for changes in model parameters impacting conductances as it steps forward in time.
- It is driven with topside precipitation maps of total precipitation energy, Q , and characteristic energy, E_0 covering impact ionization via calculations described by Fang et al. (2010).
- Additionally, the model is driven at the topside with either a map of FAC or plasma flow.
- We generate N-S cuts of these parameters and replicate these cuts along an arc contour (Clayton, 2019, 2021) with various morphologies to introduce along-arc structure.

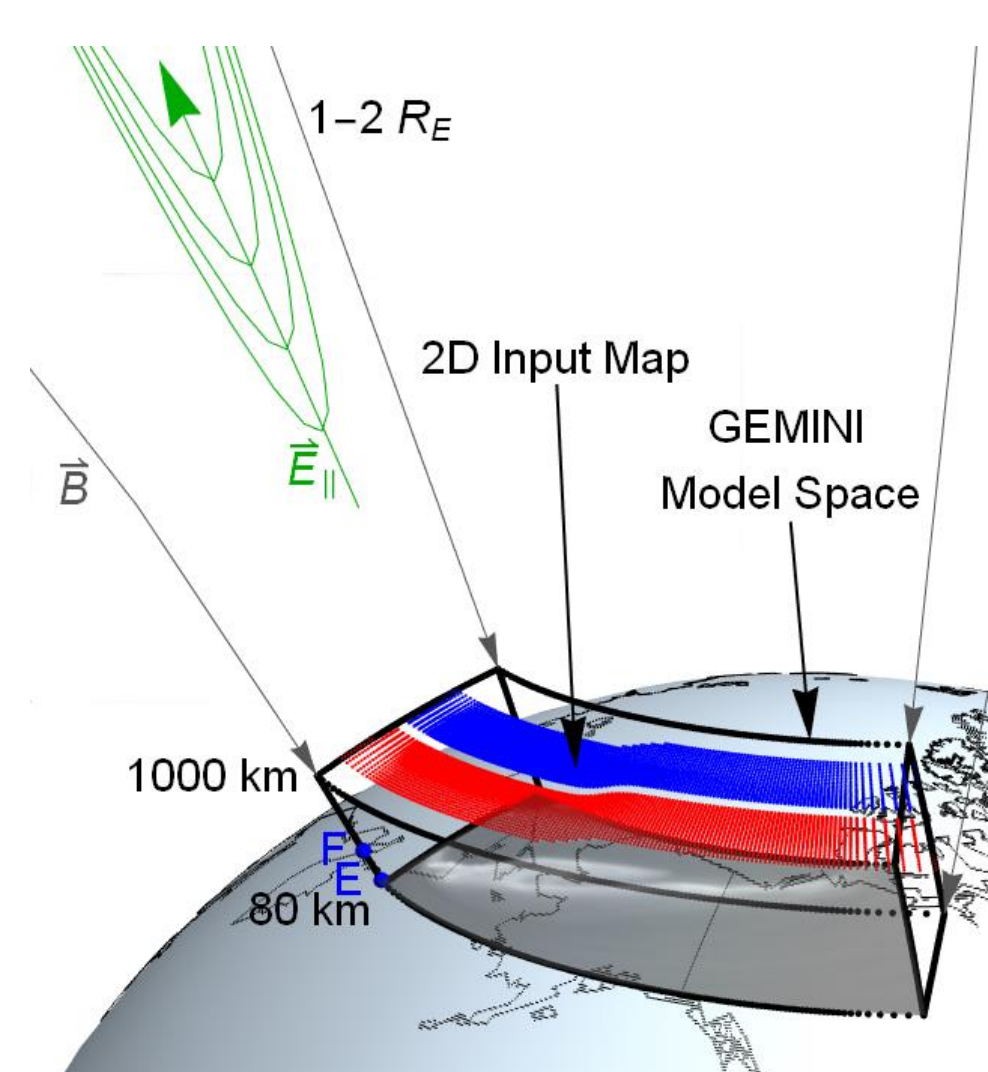


Figure 1: The general context of this work. The dotted black box depicts the GEMINI model space over Alaska. The U-shaped potential/parallel electric field is shown in green. The magnetic field lines connecting to the magnetospheric generator region are shown in gray. The top of the model space shows an example of a 2D input map of FAC and the bottom shows roughly where auroral emission lies.

Hurdle: Properly Defining Driving Maps & Determining Self-Consistency

- Determining whether we have a set of self-consistent maps of FAC, flow, and precipitation is non-trivial and starts with validating 1D, across-arc parameter cuts.
- This can be done by using
 - A) Leading order theory:**
 - Eq (1), while assuming horizontally uniform conductivity, gives a 1D solution of

$$j_{\parallel} = \pm B_0 \Sigma_P \partial v_{east} / \partial north = \pm \Sigma_P \partial E_{north} / \partial north \quad (2)$$

- Taking the opening angle $\delta B/B_0$ caused by flow shear on frozen-in field lines to be v_{east}/v_A (Mallinckrodt and Carlson, 1978), and with $v_{east} = E_{north}/B_0$ gives

$$j_{\parallel} = \pm \sqrt{\rho/\mu_0} \partial v_{east} / \partial north = \pm \Sigma_A \partial E_{north} / \partial north \quad (3)$$

- The proportionality constant here depends on the degree of quasi-statics of the system. Figure 2 shows this flow shear proportionality for two different cases.
 - B) Another way to do this** is by using in-situ and ground based data (SWARM, THEMIS-GBO), an example of which is shown in figure 3 (see poster DATA-6: "Auroral current continuity - a machine learning study using available data" by A. Mule).
 - C) A third way** is the use of literature statistical data (Wu, 2020) which can provide stereotypical parameter values, e.g., peak current densities, current sheet width, plasma flow peaks, etc.
- We use a combination of these methods to develop cartoon across-arc cuts to set ourselves up to systematically progress the model runs and interpret their data.

Hurdle: Interpretation & Visualization of 3D GEMINI Outputs

- Auroral system science is inherently 3-dimensional which would suggest a 3D approach to interpreting the model output. We do this using ParaView (Ayachit, 2015).
- Figure 4 below shows 6 GEMINI model runs described in the bottom-left table. Each of these runs are FAC driven in similar fashions as shown in Figure 2. The source line of the plasma flow and FAC streamlines are at 300 km in altitude and span +/- 200 km from the FAC inflection point. The density is cut off at a surface of a constant value of $1.1 \times 10^{11} \text{ m}^{-3}$.

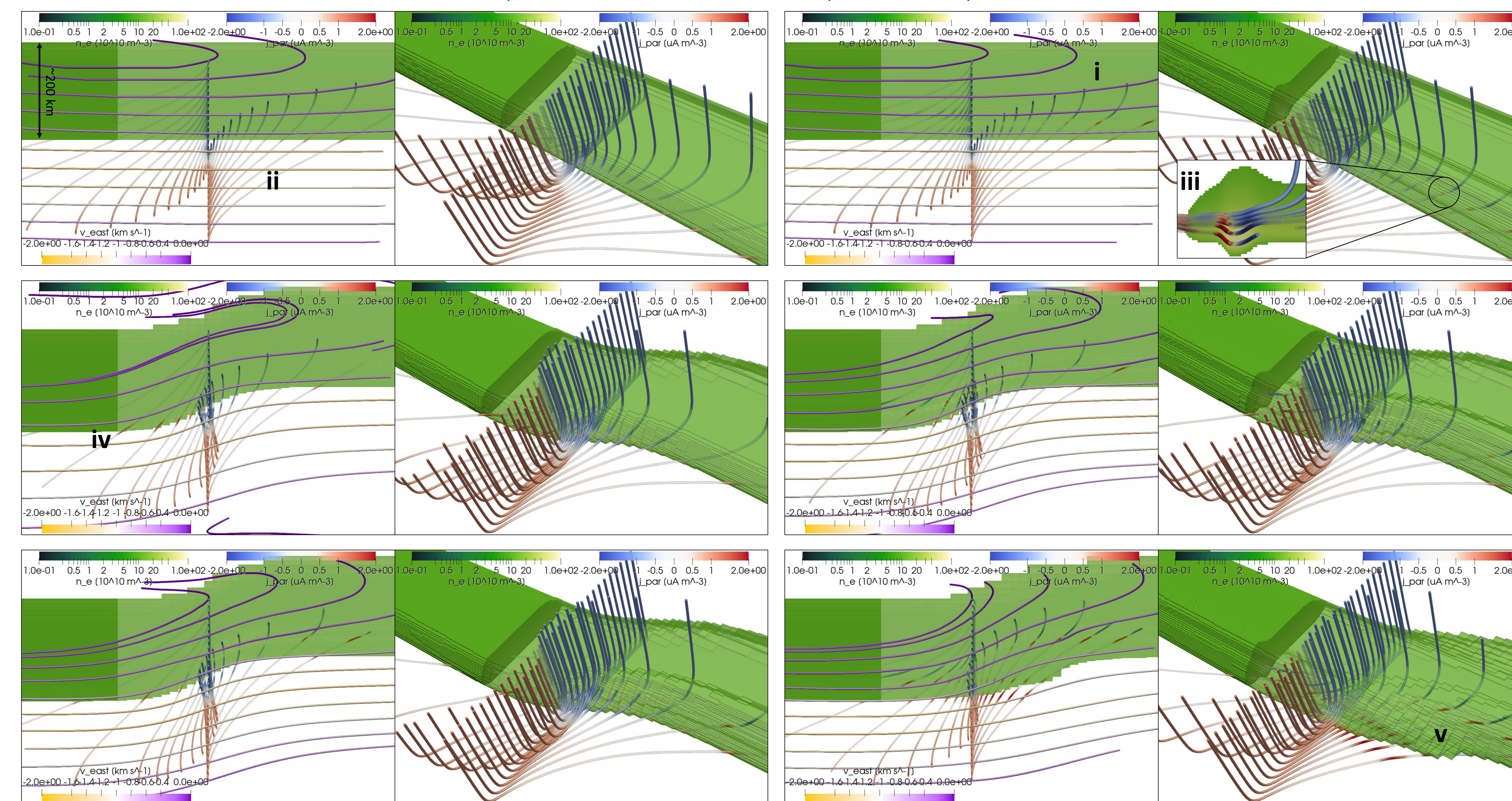


Figure 4: GEMINI renders of top views (left panel) and 3D views (right panel) of the following 6 morphologies:

BASLINE	INTENSE PRECIP.
Wide, sheet-like, medium intensity arc precip. (1 uA/m^2 , 3 keV , 3 mW/m^2)	Narrow, higher intensity precip. on top of baseline (6 keV , 15 mW/m^2)
BENT	BENT + INTENSE
Input parameters follow a minor along-arc bend	The higher energy precip. with a bend
SHARC	SURGE
A short arc; intense precip. falling off longitudinally	Bent arc that surges westward at 6 km/s

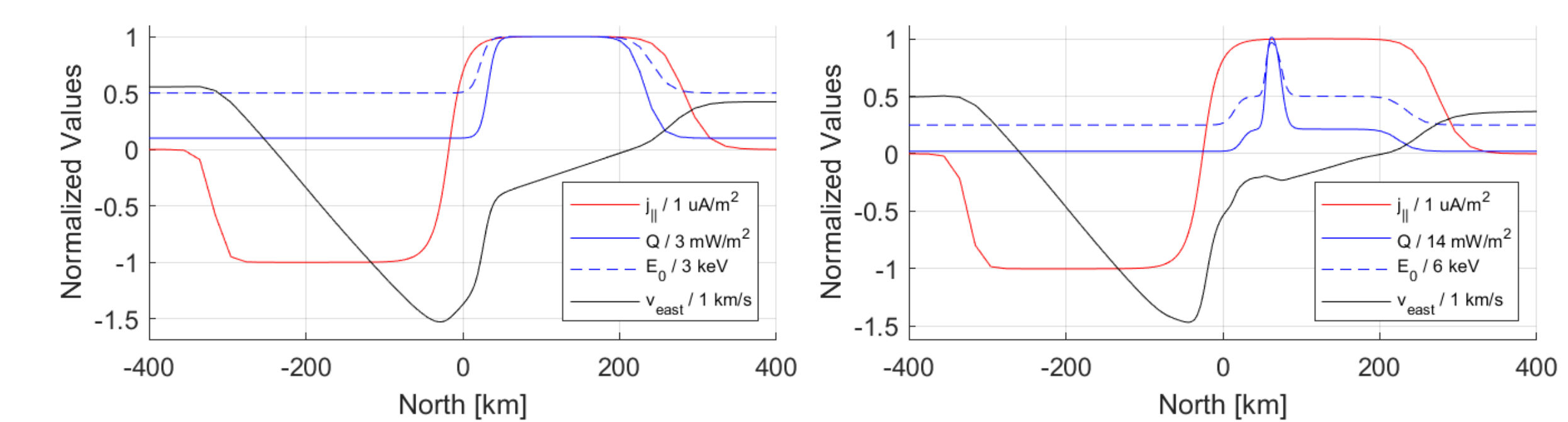


Figure 2: 1D cuts of parameter inputs, FAC (red) and precipitation (blue), against plasma flow output (black) for BASELINE (left), as defined in Figure 4, and SURGE (right). These examples show how Eqs. (2) and (3) provide reasonable first guesses for when running GEMINI flow-driven instead of FAC-driven, yet are muddled up by precipitation via conductances and their gradients.

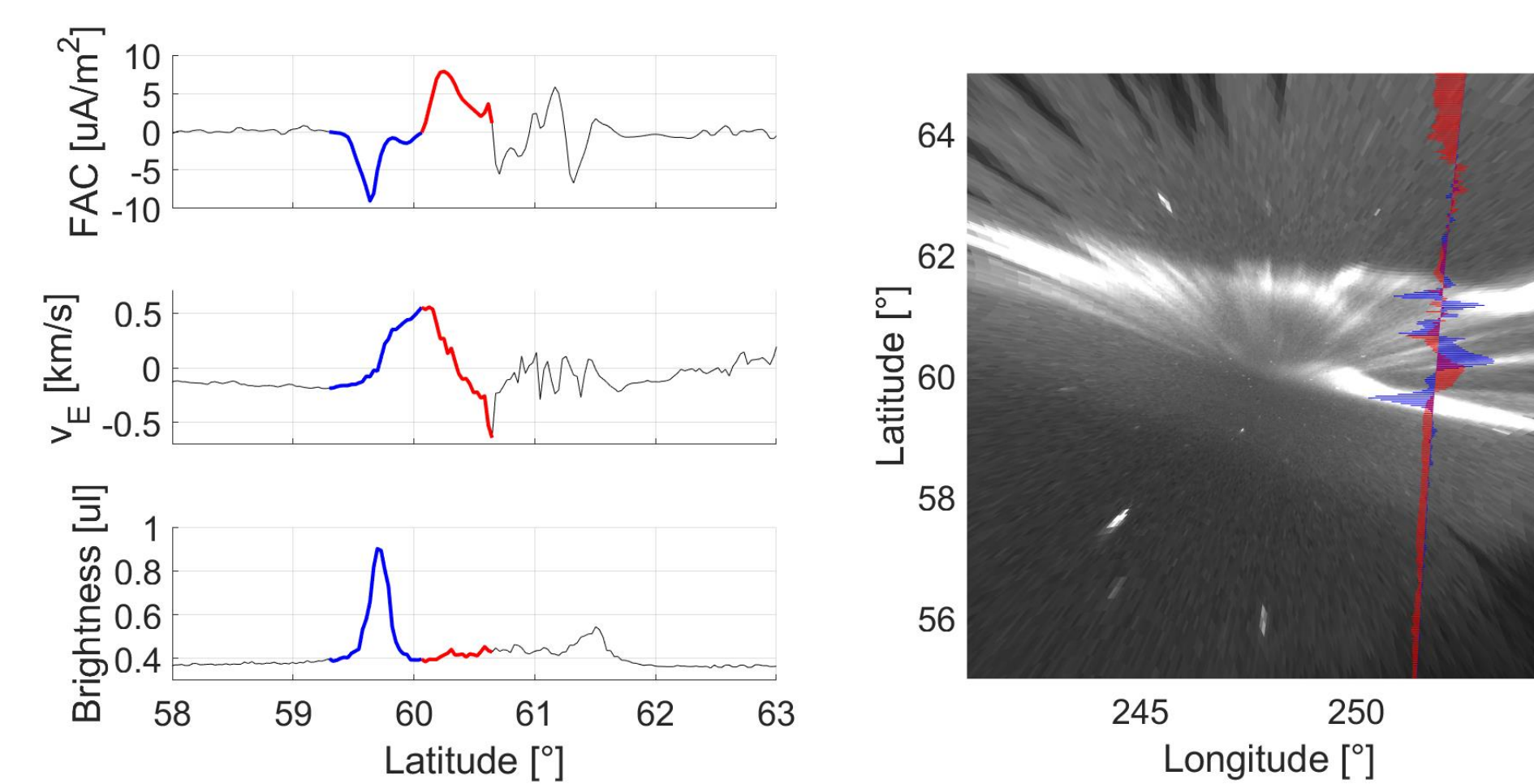


Figure 3: A stereotypical example of an up-down current pair crossing by Swarm C from April 22, 2014 along with cross-track flow data and the associated brightness provided by the Fort Smith THEMIS all-sky imager. The compilation of this figure was made using data reduced by A. Mule and M. S. Kawamura.

Discussions Contd.

- An along-arc bend causes dips of FAC at the equatorward edge of the precipitation channel.
 - This is because of a mismatch of the resulting flow contour; flow streamlines are no longer fully orthogonal to the gradients causing FAC (Eq. (1)).
- A density enhancement exists in the wake of a surging bent contour causing strong FAC signatures.
 - This is caused by finite recombination times creating a hysteresis of the precipitation in the lower ionosphere.

Conclusions

- Along-arc structure in less idealized arcs causes interesting current closure systems.
- FAC pairs closer to the current reversal latitude are dominated by Pedersen closure, while those farther away close through both Hall and Pedersen.
- Prior to connecting to FAC, horizontal currents rotate to align with the electric field, i.e., they turn into fully Pedersen currents.
- 3D visualization for less idealized auroral arcs is needed to capture the full current closure system, e.g., conclusion above, partial closure, etc.
- Longitudinal motion in bent auroral arc systems provides various hidden current closure signatures via conductance gradients caused by E-region density wakes.

Future work

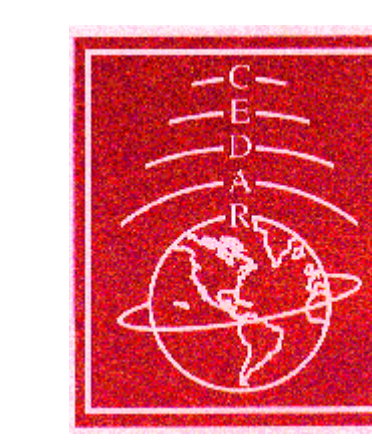
- A modular addition to GEMINI which allows for induction will be developed to allow for Alfvénic physics.
- The impact ionization calculations will be compared to inverted-V electron energy spectra to ensure proper precipitation physics.
- Additional ParaView visualization will be added such as Poynting theorem terms, or conductance gradient overlays.
- The input driver generator needs improvement in its plasma flow definition to account for Eqs. (2) and (3).
 - A table of FAC input parameters against flow shear output from GEMINI will aid in determining this proportionality of $\nabla \times \mathbf{B}$ and $\nabla \cdot \mathbf{E}$.

Acknowledgments

We would like to acknowledge and thank Dartmouth College for providing internal funding for Phase A of the Auroral Reconstruction CubeSwarm (ARCS) proposal and to NASA 80GSFC21C0009 for the ARCS MIDEX CSR funding. We would also like to thank the NSF and NASA for providing funding for the GEMINI model development from grants NSF AGS-1255181 and NASA NNX14AQ39G.

References

Wolf, R. A., 1975, *SSR*, [10.1007/BF00718584](https://doi.org/10.1007/BF00718584)
 Cowley, S. W. H., 2000, *GMS*, [10.1029/GM118p0091](https://doi.org/10.1029/GM118p0091)
 Lotko, W., 2004, *JASTP*, [10.1016/j.jastp.2004.03.027](https://doi.org/10.1016/j.jastp.2004.03.027)
 Amm, O., 2008, *AG*, [10.5194/angeo-26-3913-2008](https://doi.org/10.5194/angeo-26-3913-2008)
 Kelley, M. C., 2009, *ES*, ISBN: 9780080916576
 Marghitu, O., 2012, *GMS*, [10.1029/2011GM001189](https://doi.org/10.1029/2011GM001189)
 Kaeppler, S. R., 2012, *GMS*, [10.1029/2011GM001177](https://doi.org/10.1029/2011GM001177)
 Zettergren, M. & Semeter J., 2012, *JGR*, [10.1029/2012JA017637](https://doi.org/10.1029/2012JA017637)
 Zettergren, M. & Snively J., 2019, *JGR*, [10.1029/2018GL015699](https://doi.org/10.1029/2018GL015699)
 Fang, X., 2010, *GRL*, [10.1029/2010GL045406](https://doi.org/10.1029/2010GL045406)
 Clayton, R., 2019, *JGR*, [10.1029/2018JA026440](https://doi.org/10.1029/2018JA026440)
 Clayton, R., 2021, *JGR*, [10.1029/2021JA029749](https://doi.org/10.1029/2021JA029749)
 Mallinckrodt, A. J., 1978, *JGR*, [10.1029/JA083iA04p01426](https://doi.org/10.1029/JA083iA04p01426)
 Wu, J., 2020, *UoC*, [Unpublished doctoral thesis](https://doi.org/10.1029/2018GL015699)
 Ayachit, U., 2015, *Kitware*, ISBN: 9781930934306



CEDAR
2022 Workshop
June 19-24